

One-step covalent grafting of Fe₄ single-molecule magnet monolayers on gold

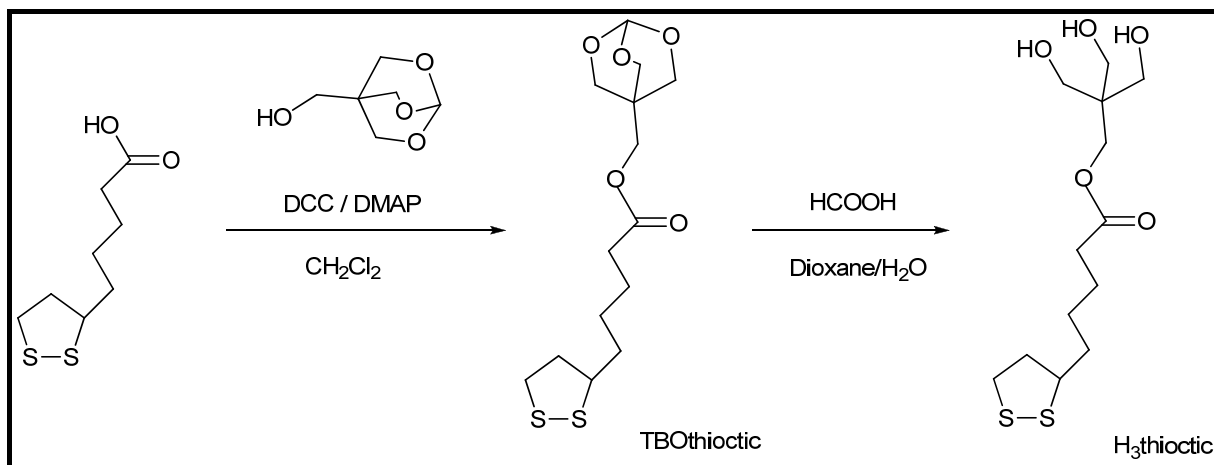
Maria Jesus Rodriguez-Douton, Matteo Mannini, Lidia Armelao, Anne-Laure Barra, Erik Tancini,
Roberta Sessoli, and Andrea Cornia*

Electronic Supplementary Information

1. General Methods

Starting materials and reagents were purchased from Aldrich and used as received unless otherwise stated. Anhydrous diethyl ether, pre-treated over CaCl_2 , was distilled from Na/benzophenone under nitrogen shortly before use. Methanol was carefully dried by treatment with Mg/I_2 and distilled prior to use. Compounds $[\text{Fe}_4(\text{OMe})_6(\text{dpm})_6]$ (**2**)¹ and 2,6,7-trioxabicyclo[2.2.2]octan-4-yl-methanol (**TBO**)² were prepared as described elsewhere. Chromatographic purification was performed using silica gel (60 Å, 200-400 mesh). All the synthesized organic compounds were confirmed by thin-layer chromatography (TLC) performed on a silica gel glass plate (Merck 60 F254). Elemental analysis was carried out on a Carlo Erba EA1110 CHNS-O automatic analyzer. ¹H and ¹³C NMR spectra were recorded at 302 K with a Bruker FT-DPX200 NMR spectrometer. Proton chemical shifts are given in ppm relative to TMS.

2. Synthesis



Scheme S1

To a stirred solution of thioctic acid (0.25 g, 1.211 mmol) in 8 mL of dry degassed CH_2Cl_2 , **TBO** (0.184 g, 1.263 mmol) was added as a solid in one portion under N_2 . The solution was cooled down to 0°C, and *N,N'*-dicyclohexylcarbodiimide (DCC, 0.499 g, 2.42 mmol) and a catalytic amount of 4-dimethylaminopyridine (DMAP, 14.78 mg, 0.121 mmol) were added. The reaction was stirred for 4 hours, slowly warmed up to room temperature and stirred for another 14 hours. The white precipitate formed (*N,N'*-dicyclohexylurea, DCU, 0.27 g) was filtered out and the solvent was removed *in vacuo* to give, according to ¹H NMR analysis, the intermediate 2,6,7-trioxabicyclo[2.2.2]octan-4-ylmethyl 5-(1,2-dithiolan-3-yl)pentanoate (**TBOnthioctic**) as a yellow oil *plus* unreacted DCC (0.661 g, 99%). This mixture was dissolved in 1,4-dioxane (7.5 mL) and H_2O (15 mL), and was acidified with formic acid, 98% (0.142 mL, 3.76 mmol) until pH = 5 to accomplish acid deprotection. The suspension was stirred at 60°C for 5 days, following the evolution of the reaction by TLC (SiO_2 , $\text{CH}_2\text{Cl}_2/\text{MeOH}$, 9:1), until complete liberation of the trimethylol function. The solid was filtered, and the solvent was removed *in vacuo*. The crude material was purified with column chromatography on silica gel [SiO_2 : $\text{CH}_2\text{Cl}_2/\text{MeOH}$ (9:1)] to give pure **H₃thioctic** as a yellow oil (0.099 g, 0.305 mmol, 25%).

¹H NMR for **TBOthioctic**; δ_H (200 MHz; CDCl₃, Me₄Si) 1.41-1.59 (2 H, m), 1.63-1.77 (4 H, m), 1.83-1.99 (1 H, m), 2.35 (2 H, t, J=7.5 Hz), 2.42-2.54 (1 H, m), 3.08-3.25 (2 H, m), 3.50-3.63 (1 H, m), 3.88 (2 H, s), 4.00 (6 H, s), 5.56 (1 H, s).

¹H NMR for **H₃thioctic**; δ_H (200 MHz; CD₃OD, Me₄Si) 1.14-1.29 (2 H, m), 1.43-1.77 (4 H, m), 1.82-1.98 (1 H, m), 2.37 (2 H, t, J=7.5 Hz), 2.39-2.55 (1 H, m), 3.04-3.25 (2 H, m), 3.31 (3 H, br), 3.51-3.65 (1 H, m), 3.58 (6 H, s), 4.10 (2H, s). ¹³C NMR for **H₃thioctic**; δ_C (200 MHz; CD₃OD, Me₄Si) 24.36, 28.39, 33.45, 34.32, 37.92, 39.88, 44.82, 56.10, 61.11, 62.84, 174.01. Anal. Calc. for **H₃thioctic**, C₁₃H₂₄O₅S₂: C, 48.12; H, 7.46; S, 19.77. Found: C, 48.44; H, 7.04; S, 19.44%.

[Fe₄(thioctic)₂(dpm)₆] (**1**). To a stirred solution of **2** (0.040 g, 0.027 mmol) in 15 mL of dry diethyl ether, **H₃thioctic** (0.023 g 0.072 mmol) in 2 mL of dry diethyl ether was added, and the mixture was stirred for two hours. Vapour diffusion of dry methanol (35 mL) into the clear solution at room temperature afforded dark orange crystals, which were collected by filtration and washed with the external solution and with anhydrous methanol, and finally dried under vacuum (0.036 g, 68%). Anal. Calc. for C₉₂H₁₅₆Fe₄O₂₂S₄: C, 56.21; H, 8.00; S, 6.52. Found: C, 56.53; H, 7.73; S, 6.61%.

3. X-Ray Diffraction

Crystals of **1** were analyzed at 120(2) K on an Oxford Diffraction Xcalibur3 four-circle diffractometer using Mo-K_α radiation and Cryostream 600 low-temperature device. The unit cell was found to be metrically trigonal, with *a* = 31.9958(9) Å and *c* = 54.8101(17) Å (*R*(obv) lattice in hexagonal setting). The symmetry of the diffraction pattern was consistent with Laue class -3m1 (*R*_{merge} = 0.045) and systematic absences clearly pointed to space group *R*-3c (in reflections *h*0*l*, <*I*/*σ(I)*> = 30.68 for *l* = 2*n* and 0.06 for *l* = 2*n*+1). However, all tested crystals diffracted very weakly at high angles (<*I*/*σ(I)*> = 1.79 for θ = 17.6-19.1°), as confirmed by the high value of *U*(mean) = 0.061 Å² in Wilson plot. The structure could be solved in space group *R*-3c, with the tetrairon(III) complexes developing around twofold axes perpendicular to *c*. The terminal portion of the alkyl chain was very difficult to locate in Δ*F* maps. The CH₂OC(O)CH₂ moiety could be reasonably well fitted using unit occupancies, but only 30-50% of the remaining (CH₂)₃(C₃H₅S₂) group was found to be ordered (though with very large displacements for the terminal five-membered ring). These disorder effects, which prevented a satisfactory refinement of the structure, may be in part related to the fact that thioctic acid is a racemic mixture.

4. Direct current (DC) magnetic data

DC magnetic data for a polycrystalline sample of **1** (23.54 mg) pressed in a pellet and wrapped in Teflon tape were recorded on a Cryogenic S600 SQUID magnetometer. Magnetization (*M*) was measured in applied fields (*H*) of 1 kOe from 1.9 to 35 K and 10 kOe from 35 K to 300 K and magnetic susceptibility was evaluated as *M/H*. Isothermal *M* vs. *H* curves were also measured at 1.9, 2.5 and 4.5 K in fields up to 50 kOe.

The measured data, corrected for the sample holder contribution, were reduced using a molecular weight of 1965.87 and a diamagnetic contribution (estimated from Pascal's constants) of $-1127 \cdot 10^{-6}$ emu/mol.

Molar susceptibility (χ_m) data, shown in Figure S1 as a $\chi_m T$ vs. T plot, have been fitted using the exchange + Zeeman spin Hamiltonian

$$\hat{\mathbf{H}} = J \hat{\mathbf{S}}_1 \cdot (\hat{\mathbf{S}}_2 + \hat{\mathbf{S}}_3 + \hat{\mathbf{S}}_4) + J' (\hat{\mathbf{S}}_2 \cdot \hat{\mathbf{S}}_3 + \hat{\mathbf{S}}_3 \cdot \hat{\mathbf{S}}_4 + \hat{\mathbf{S}}_4 \cdot \hat{\mathbf{S}}_2) + \mu_B g \hat{\mathbf{S}} \cdot \hat{\mathbf{H}} \quad (\text{S1})$$

(1 is the central Fe^{3+} ion; 2, 3, and 4 label the peripheral Fe^{3+} ions, each with spin $S_i = 5/2$; \mathbf{S} is the total spin). The best fit parameters were $J = 16.32(9)$ cm $^{-1}$, $J' = 0.23(6)$ cm $^{-1}$, $g = 1.979(2)$, with a Curie-Weiss correction $\theta = -0.129(15)$ K to phenomenologically reproduce the drop of the $\chi_m T$ product at $T < 10$ K. Isothermal M_m vs. H data (Fig. S1, inset) were accurately fitted using an axial zero-field splitting Hamiltonian

$$\hat{\mathbf{H}}_{\text{zfs}} = \mu_B \hat{\mathbf{S}} \cdot \hat{\mathbf{H}} + D [\hat{S}_z^2 - S(S+1)/3] \quad (\text{S2})$$

with $S = 5$, $D = -0.419(4)$ cm $^{-1}$ and $g = 1.983(2)$. An accurate fit was not possible by imposing $D > 0$.

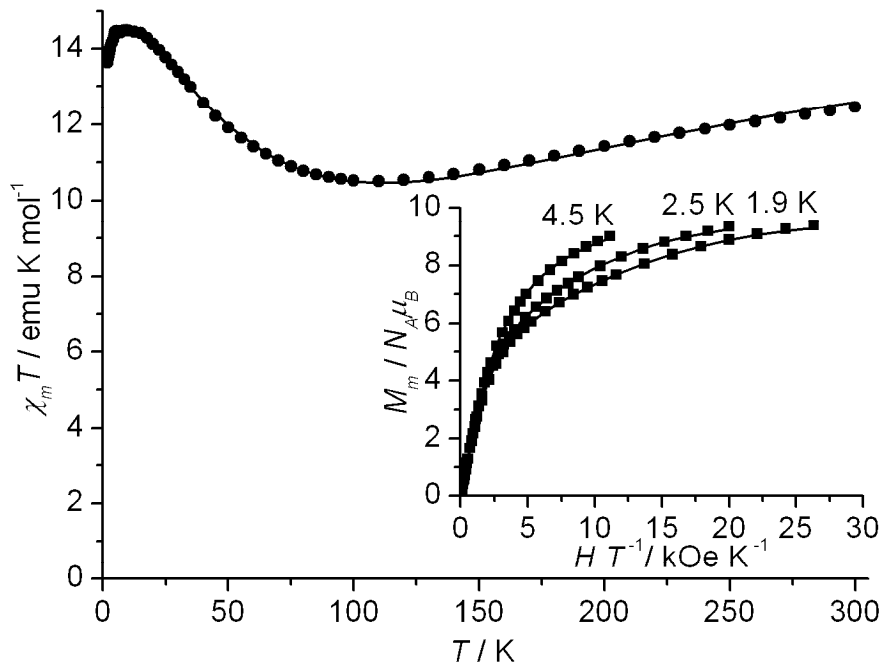


Fig. S1. DC magnetic data for **1**, with best fit calculated curves (solid lines). The main panel displays $\chi_m T$ vs. T data, while the inset shows M_m vs. H/T data recorded at three temperatures.

5. Alternating current (AC) magnetic data

The AC magnetic susceptibility of **1** in zero static field was measured in the frequency range $\nu = 100$ -70000 Hz at several temperatures in the 1.6 - 4.5 K range on a microcrystalline powder sample of **1** using a home made AC susceptometer based on the Oxford Instruments MAGLAB2000 platform. Data reduction was carried out as described for DC data. The frequency dependence of the out-of-phase susceptibility, χ'' , at each temperature was fitted using the extended Debye model to take into account the possible distribution of relaxation times according to:

$$\chi''(\omega) = (\chi_T - \chi_S) \frac{(\omega\tau)^{1-\alpha} \cos(\alpha\pi/2)}{1 + 2(\omega\tau)^{1-\alpha} \sin(\alpha\pi/2) + (\omega\tau)^{2-\alpha}} \quad (\text{S3})$$

where χ_T and χ_S are the isothermal and adiabatic susceptibilities, respectively, τ is the relaxation time, $\omega = 2\pi\nu$, and α the parameter describes the width of the distribution of relaxation times.

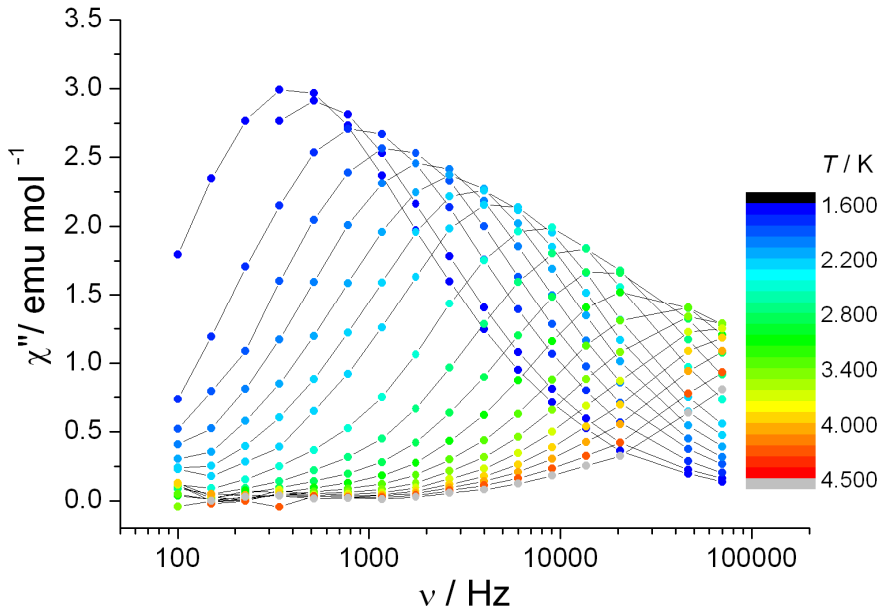


Fig. S2. Out-of-phase component of the AC magnetic susceptibility of **1** measured in zero static field.

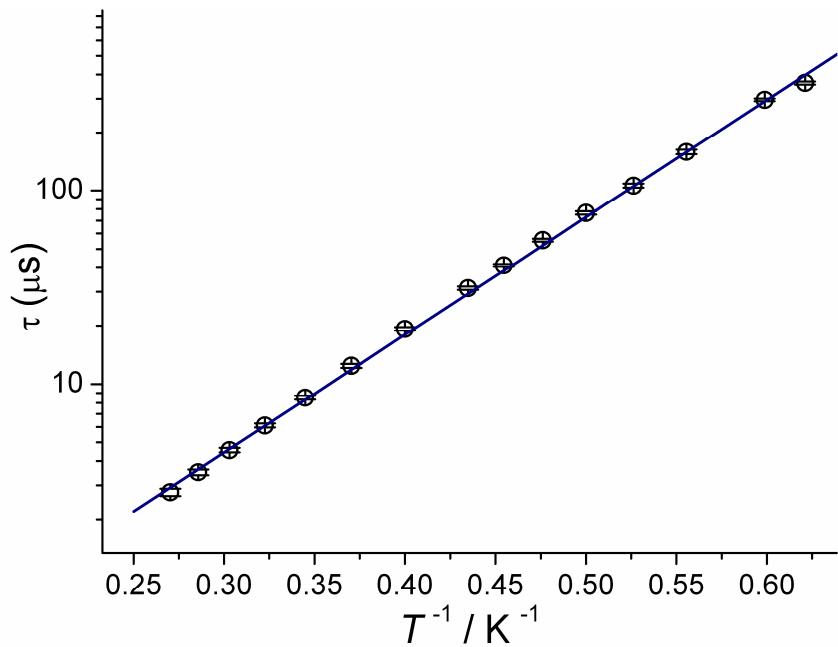


Fig. S3. Relaxation time of the magnetization of **1** as a function of reciprocal temperature. The line provides the best fit to experimental data using Arrhenius law $\tau = \tau_0 \exp(U_{\text{eff}}/k_B T)$ with $\tau_0 = 6.6(3) \cdot 10^{-8}$ s and $U_{\text{eff}}/k_B = 14.0(1)$ K.

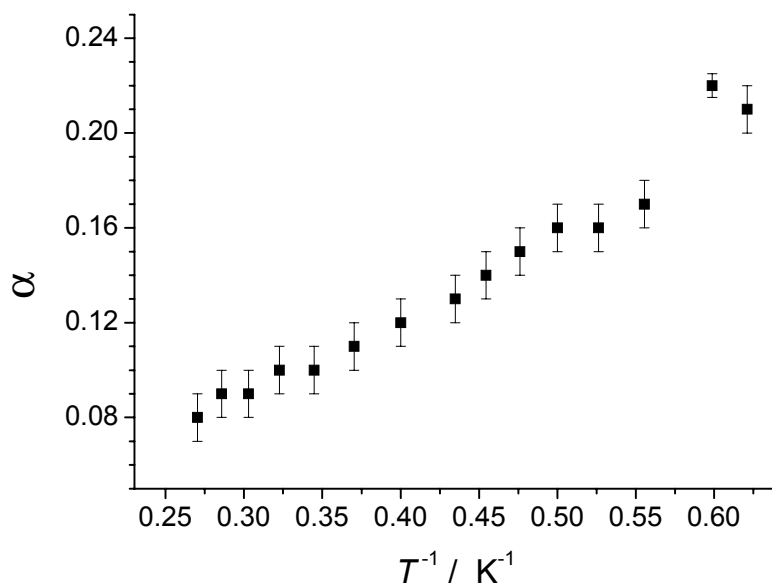


Fig. S4. Temperature dependence of the width of the distribution of relaxation times described by the α parameter in Eq. S3.

6. High-Frequency EPR (HF-EPR)

HF-EPR spectra were recorded on a homebuilt spectrometer³ working in transmission, at 5, 10 and 20 K. Gunn diodes operating at 95 GHz or 115 GHz, equipped with a frequency doubler, were used as source excitation. A Quasi-Optical table propagates the exciting light outside the cryostat, whereas a corrugated waveguide is used inside the cryostat. A small modulating field is added to the main magnetic field in order to measure the derivative of the light transmitted through the sample. The detection is performed with a hot electron InSb bolometer.

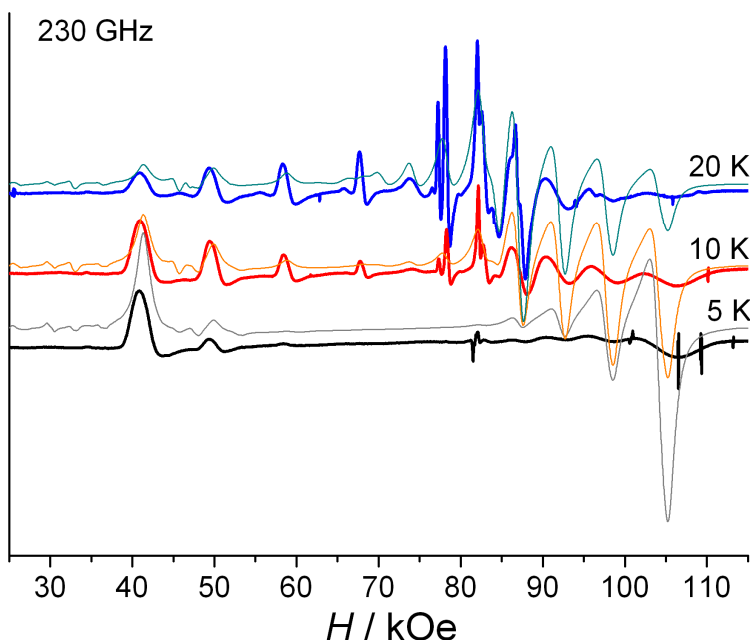


Fig. S5. Experimental (bold lines) and simulated (thin lines) HF-EPR spectra of **1** at 230 GHz and three temperatures.

7. X-Ray Photoelectron Spectroscopy

XP spectra were recorded on a Perkin–Elmer Φ 5600ci spectrometer using a non monochromatized (15 kV, 300 W) Al K_α radiation (1486.6 eV). The sample analysis area was 2 mm in diameter, and the working pressure was lower than 10⁻⁹ mbar. The spectrometer was calibrated assuming the binding energy (BE) of the Au4f_{7/2} line at 83.9 eV with respect to Fermi level. The standard deviation for the BEs was ±0.15 eV. Bulk crystalline **1** was mounted on steel sample holders and introduced directly into the XPS analytical chamber by a fast entry lock system. Monolayers were prepared and mounted on sample holders under dry nitrogen environment in a portable glove bag which was then directly connected to the fast entry system of the XPS vacuum chamber in order to minimize air exposure and atmospheric contamination. Survey scans were run in the 0–1300 eV range to identify the chemical species present in the samples. Detailed scans were recorded for the C1s, O1s, S2s, S2p, Fe2p and Au4f photo-peaks. For bulk crystalline **1**, BE shifts due to charging effects were corrected assigning to the adventitious C1s line a BE of 284.8 eV.⁴ Monolayers were sufficiently electrically conductive at room temperature that no compensation for charging effects was required. The analysis involved Shirley-type background subtraction and, whenever necessary, spectral deconvolution, which was carried out by non-linear least-squares curve fitting, adopting a Gaussian-Lorentzian sum function. The atomic composition of the samples was calculated by peak integration, using sensitivity factors provided by the spectrometer manufacturer (Φ V5.4A software) and taking into account the geometric configuration of the apparatus. The results of the analysis are gathered in Tables S1–S4. The experimental uncertainty on the reported atomic composition values does not exceed ± 5%.

Table S1. XPS data recorded on monolayers of **1** on Au(111), and expected composition

Monolayer	BE (eV)	FWHM (eV)	% at.	Calcd % at. ^a
C1s	284.8	2.4	72.9	75.4
O1s	531.8	2.8	20.2	18.0
S2p	162.0	2.7	3.3	3.3
Fe2p _{3/2}	711.0	--	3.6	3.3
S2s	226.2	3.1	--	--
Au4f _{7/2}	83.9	1.6	--	--

^a for C₉₂Fe₄O₂₂S₄

Table S2. Deconvolution of C1s XPS peak recorded on monolayers of **1** on Au(111)

Monolayer C1s	BE (eV)	FWHM (eV)	% at.
C _I	284.8	1.9	72.0
C _{II}	286.4	2.0	22.1
C _{III}	288.9	2.1	5.9

Table S3. XPS data recorded on bulk crystalline **1**

Bulk	BE (eV)	FWHM (eV)
C1s	284.8	2.4
O1s	531.8	3.0
S2p	163.6	2.9
Fe2p _{3/2}	711.1	--
S2s	227.8	3.3

Table S4. Deconvolution of C1s XPS peak recorded on bulk crystalline **1**

Bulk C1s	BE (eV)	FWHM (eV)	% at.
C _I	284.8	1.9	81.5
C _{II}	286.5	1.9	14.7
C _{III}	289.0	2.0	3.8

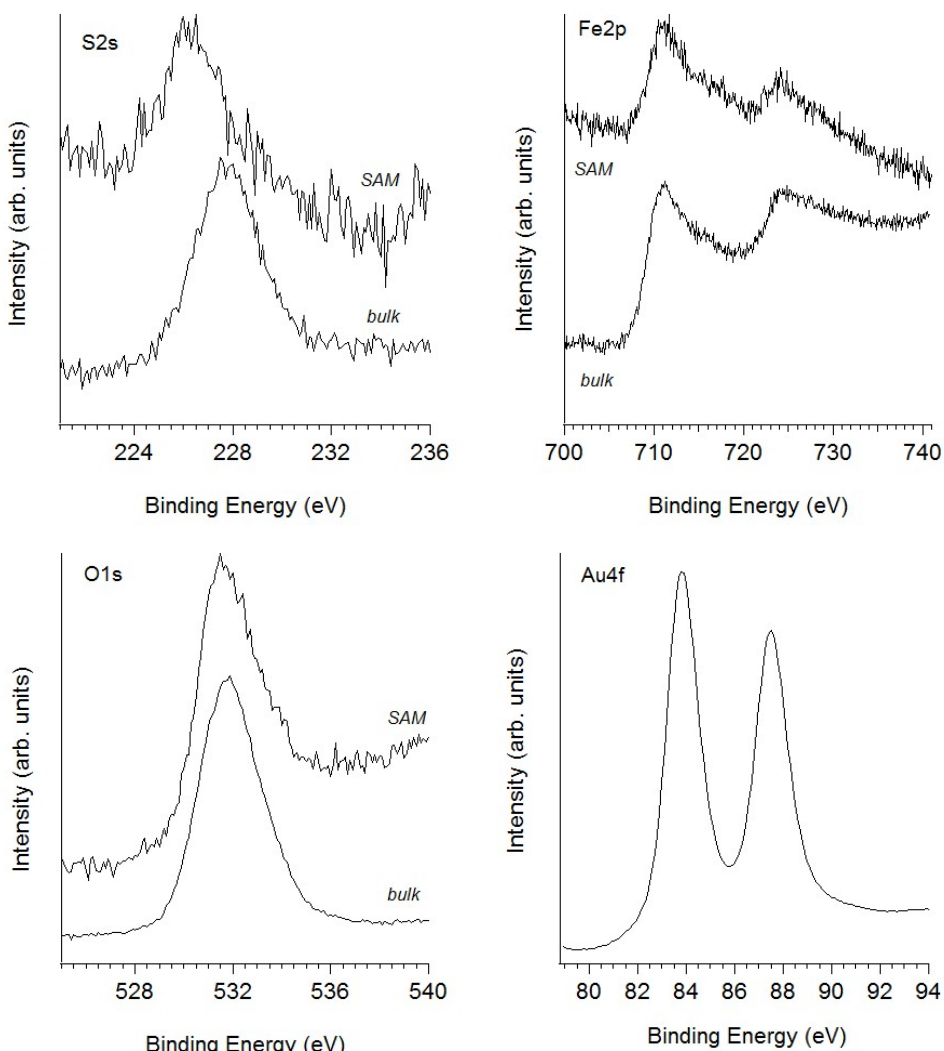


Fig. S6. Comparison between S2s, Fe2p and O1s XPS peaks recorded on bulk and monolayer samples of **1**, and Au4f peak detected on monolayers.

8. STM experiments

Morphological analysis has been carried out with a NT-MDT Solver P47pro Scanning Tunneling Microscope (NT-MDT, Zelenograd, Moscow, Russia; www.ntmdt.ru) equipped with a custom built low-current head operated in nitrogen gas atmosphere. Tips were prepared by mechanical sharpening of Pt/Ir 90:10 wire. The image analysis has been carried out with the WSXM 5.2 software from Nanotec (Spain).⁵ Statistical analysis of the extracted diameters has been performed with the Origin 8.1 suite from OriginLab.

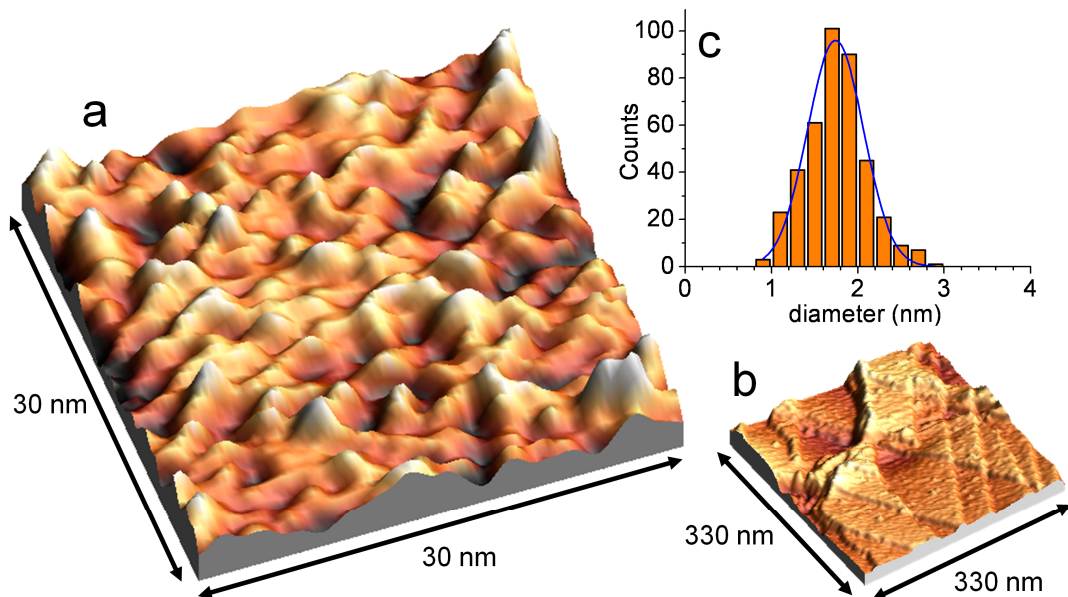


Fig. S7. (a and b) STM scans recorded on a monolayer of **1** on gold, evidencing Au(111) reconstruction and molecular features. Experimental conditions: tunnelling current 5 pA, bias voltage 840 mV. (c) Size statistics over ca. 400 objects found in three independent image scans.

9. XAS and XMCD experimental details

Fe L_{2,3} edge X-ray absorption spectra were recorded at the SIM beamline⁶ of the Swiss Light Source (SLS) using the TBT-XMCD endstation setup⁷ equipped with a pumped ⁴He cryostat. The experimental setup consists of a split coil superconducting magnet which provides magnetic fields up to 7 T in a direction parallel or antiparallel to the X-ray beam. The sample was mounted in a cold finger which allows to cool the sample down to 2 K. All X-ray measurements were made under UHV conditions ($\sim 10^{-10}$ mbar). Absorption spectra were collected in the total electron yield (TEY) mode in order to achieve the surface sensitivity required to detect signals from monolayers and following the procedure we established for SMMs to avoid radiation damaging.^{8,9} For the XMCD experiments we used one of the two APPLE-2 type undulators of the beamline (ID2) producing circular polarized X-rays with a polarization rate close to 100%. XAS spectra were recorded using both positive and negative magnetic field (parallel and antiparallel to the propagation vector of the X-rays) for both left (σ^+) and right (σ^-) circular polarization, in order to minimize systematic errors (in the dipolar approximation, reversing the magnetic field is equivalent to changing the helicity of the beam¹⁰). The dichroic contribution (XMCD) has been evaluated as $(\sigma^- - \sigma^+)$ and expressed as percentage of the edge-jump of the isotropic signal $(\sigma^- + \sigma^+)/2$.

10. References

- 1 S. Accorsi, A. L. Barra, A. Caneschi, G. Castanet, A. Cornia, A. C. Fabretti, D. Gatteschi, C. Mortalo, E. Oliveri, F. Parenti, P. Rosa, R. Sessoli, L. Sorace, W. Wernsdorfer and L. Zobbi, *J. Am. Chem. Soc.*, 2006, **128**, 4742.
- 2 (a) A. B. Padias and H. K. Hall, *Macromolecules*, 1982, **15**, 217; (b) A. B. Padias, H. K. Hall, D. A. Tomalia and J. R. McConnell, *J. Org. Chem.*, 1987, **52**, 5305.
- 3 A. L. Barra, A. K. Hassan, A. Janoschka, C. L. Schmidt and V. Schünemann, *Appl. Magn. Reson.*, 2006, **30**, 385.
- 4 D. Briggs and M. Seah, *Practical Surface Analysis 2nd Edn., Vol. 1, Auger and X-Ray Photoelectron Spectroscopy*, Wiley, Chichester, 1990.
- 5 I. Horcas, R. Fernandez, J.M. Gomez-Rodriguez, J. Colchero, J. Gomez-Herrero and A.M. Baro, *Rev. Sci. Instr.*, 2007, **78**, 013705.
- 6 U. Flechsig, F. Nolting, A. Fraile Rodriguez, J. Krempasky, C. Quitmann, T. Schmidt, S. Spielmann and D. Zimoch, *AIP Conf. Proc.*, 2010, **1234**, 319.
- 7 P. Sainctavit and J.-P. Kappler, *Magnetism and Synchrotron Radiation, Lecture Notes in Physics*, Vol. 565, Springer, Berlin, 2001.
- 8 M. Mannini, F. Pineider, Ph. Sainctavit, C. Danieli, E. Otero, C. Sciancalepore, A. M. Talarico, M.-A. Arrio, A. Cornia, D. Gatteschi and R. Sessoli, *Nat. Mater.*, 2009, **8**, 194.
- 9 M. Mannini, F. Pineider, Ph. Sainctavit, L. Joly, A. Fraile-Rodriguez, M.-A. Arrio, Ch. Cartier dit Moulin, W. Wernsdorfer, A. Cornia, D. Gatteschi and R. Sessoli, *Adv. Mater.*, 2009, **21**, 167.
- 10 C. Brouder and J.-P. Kappler, *Magnetism and Synchrotron Radiation, Lecture Notes*, Les éditions de physique, 1997.